DOI: 10.2478/jwld-2013-0001

JOURNAL OF WATER AND LAND DEVELOPMENT
J. Water Land Dev. 2013, No. 18 (I–VI): 3–12
PL ISSN 1429–7426
Available (PDF): www.itep.edu.pl/wydawnictwo; http://versita.com/jwld/

Received 19.11.2012
Reviewed 24.01.2013
Accepted 28.01.2013

A – study design
B – data collection
C – statistical analysis
D – data interpretation
E – manuscript preparation
F – literature search

Drought forecasting using new machine learning methods

Anteneh BELAYNEH [ABCDEF], **Jan ADAMOWSKI** [ABCDEF]

Department of Bioresource Engineering, Faculty of Agricultural and Environmental Sciences, McGill University, Quebec, Canada, H9X 3V9; e-mail: jan.adamowski@mcgill.ca

For citation: Belayneh A., Adamowski J. 2013. Drought forecasting using new machine learning methods. Journal of Water and Land Development. No. 18 p. 3–12.

Abstract

In order to have effective agricultural production the impacts of drought must be mitigated. An important aspect of mitigating the impacts of drought is an effective method of forecasting future drought events. In this study, three methods of forecasting short-term drought for short lead times are explored in the Awash River Basin of Ethiopia. The Standardized Precipitation Index (*SPI*) was the drought index chosen to represent drought in the basin. The following machine learning techniques were explored in this study: artificial neural networks (ANNs), support vector regression (*SVR*), and coupled wavelet-ANNs, which pre-process input data using wavelet analysis (WA). The forecast results of all three methods were compared using two performance measures (*RMSE* and R^2). The forecast results of this study indicate that the coupled wavelet neural network (WA-ANN) models were the most accurate models for forecasting *SPI* 3 (3-month *SPI*) and *SPI* 6 (6-month *SPI*) values over lead times of 1 and 3 months in the Awash River Basin in Ethiopia.

Key words: *agriculture, artificial neural networks, drought forecast, SPI, support vector regression, wavelet analysis*

INTRODUCTION

One of the major challenges of agricultural systems is how to mitigate the impacts of droughts. Droughts impact agricultural systems economically as well as environmentally. With respect to economic impacts, droughts damage agricultural production, and can cause economic damage to industries connected to agricultural production, in addition to causing unemployment as a result of reduced production. From an environmental perspective, droughts can deprive crops and soils of essential precipitation as well as increase the salt content in soils and irrigation systems [MISHRA, SINGH 2010].

To mitigate the impacts of drought an effective and timely monitoring system is required. Effective monitoring of droughts can aid in developing an early warning system. An objective evaluation of the drought condition in a particular area is the first step for planning water resources in order to prevent and mitigate the impacts of future occurrences of drought. The evaluation and forecasting of drought is made possible by the use of drought indices. There are several drought indices that are commonly used, such as the Palmer Index, the Crop Moisture Index and the Standardized Precipitation Index (*SPI*). The Palmer Index and the *SPI* are traditionally the most popular indices for forecasting drought due to their standardization. For the purposes of comparing drought conditions from different areas, which often have different hydrological balances, the most important characteristic of a drought index is its standardization [BONNACCORSO *et al*. 2003]. Standardization of a drought in-

dex ensures independence from geographical position as the index in question is calculated with respect to the average precipitation in the same place [CACCIAMANI *et al*. 2007].

One of the differences between the Palmer Index and the SPI is that the characteristics of the Palmer Index vary from site to site while those of the *SPI* do not. Another difference is the Palmer Index has a complex structure with a very long memory, while the *SPI* is an easily interpreted, simple moving average process [TSAKIRIS, VANGELIS 2004]. This characteristic makes the *SPI* useful as the primary drought index because it is simple, spatially invariant in its interpretation and probabilistic, allowing it to be used in risk and decision making analysis. The *SPI* is also more representative of short-term precipitation than the Palmer Index and is thus a better indicator for soil moisture variation and soil wetness [MISHRA, SINGH 2010]. Given the focus of this paper on short-term drought, this characteristic makes the use of the *SPI* more advantageous. The *SPI* also provides a better spatial standardization than does the Palmer Index with respect to extreme drought events [LLOYD-HUGHES, SAUNDERS 2002]. The *SPI* has also been found to be better than the Palmer Index in detecting the onset of a drought event [HAYES 1996]. Given the aforementioned advantages of the *SPI* over the Palmer Index, the *SPI* was the drought index chosen to forecast in this study.

The *SPI* will be forecast using machine learning models in this study, namely artificial neural networks (ANN) and support vector regression models (SVR), respectively. These machine learning or data driven models have become increasingly popular in hydrologic forecasting because they are effective in dealing with the non-linear characteristics of hydrologic data. ANNs have been used to forecast droughts in several studies [BACANLI *et al*. 2008; BARROS, BAWDEN 2008; CUTORE *et al*. 2009; KARAMOUZ *et al.* 2009; MARJ, MEIJERINK 2011; MISHRA, DESAI 2006; MORID *et al*. 2007]. There are several studies where SVRs were used in hydrological forecasting. KHAN and COULIBALY [2006] found that an SVR model was more effective at predicting 3–12 month lake water levels than ANN models. KISI and CIMEN [2009] used SVRs to estimate daily evaporation. Finally, SVRs have been successfully used to predict hourly streamflow [ASEFA *et al*. 2006], precipitation [KISI, CIMEN 2012], and were shown to perform better than ANN models for monthly streamflow prediction [MAITY *et al*. 2010; WANG *et al*. 2009], respectively. However, SVRs have not been directly used in drought forecasting to date.

A major limitation of both ANN and SVR models is their ability to deal with non-stationary data. To overcome this limitation, researchers have increasingly begun to use wavelet analysis to pre-process the inputs of hydrologic data. In this study, wavelet analysis was used in conjunction with an ANN model and compared to a traditional ANN model and an SVR model. Using these three models, *SPI* 3 and *SPI* 6, which are short-term agricultural drought indicators, were forecasted over lead times of 1 and 3 months, respectively. Both *SPI* 3 and *SPI* 6 were forecasted in the Awash River Basin of Ethiopia.

MATERIALS AND METHODS

THE AWASH RIVER BASIN

In this study, the *SPI* was forecast in the Awash River Basin of Ethiopia (Fig. 1). Forecasts were made and compared for two stations, the Meisso station and Hirna station, within the basin. These two stations are located within the Middle Awash Basin. The Hirna station is labeled on the map and has an elevation of 308 meters above sea level. The Meisso station is located directly west of the Hirna station at an elevation of 259 meters above sea level. While the study was conducted using all the meteorological stations, the results were presented for these two stations in detail.

Drought is a common occurrence in the Awash River Basin [EDOSSA *et al*. 2010]. Ethiopia's weather and climate are extremely variable both temporally and spatially. The heavy dependence of the population on rain-fed agriculture has made the people and the country's economy extremely vulnerable to the impacts of droughts. Current monthly and seasonal drought forecasts are done using the normalized vegetation index (*NDVI*). While the *NDVI* is an effective drought index it is sensitive to changes in vegetation and has limitations in areas where vegetation is minimal. Forecasts of *SPI* 3 and *SPI* 6 are not dependent on vegetative cover and can be used as another tool for drought forecasts within the basin and the country as a whole to complement the *NDVI* forecasts.

The mean annual rainfall of the basin varies from about 1,600 mm in the highlands to 160 mm in the northern point of the basin. The total amount of rainfall also varies greatly from year to year, resulting in severe droughts in some years and flooding in others. The total annual surface runoff in the Awash Basin amounts to some $4{,}900 \cdot 10^6$ m^3 [EDOSSA *et al*. 2010]. Effective forecasts of the *SPI* can be used for mitigating the impacts of hydrological drought that manifests as a result of rainfall shortages in the area. The climate of the Awash River Basin varies between a mild temperate climate in the Upper Awash sub-basin to a hot semi-arid climate in both the Middle and Lower sub-basins. The Awash River Basin supports farming, from the growth of lowland crops such as maize and sesame to pastoral farming practices. Rainfall records from 1970–2005 were used to generate *SPI* 3 and *SPI* 6 time series from each station. Descriptive statistics for precipitation at the two stations is shown in Table 1.

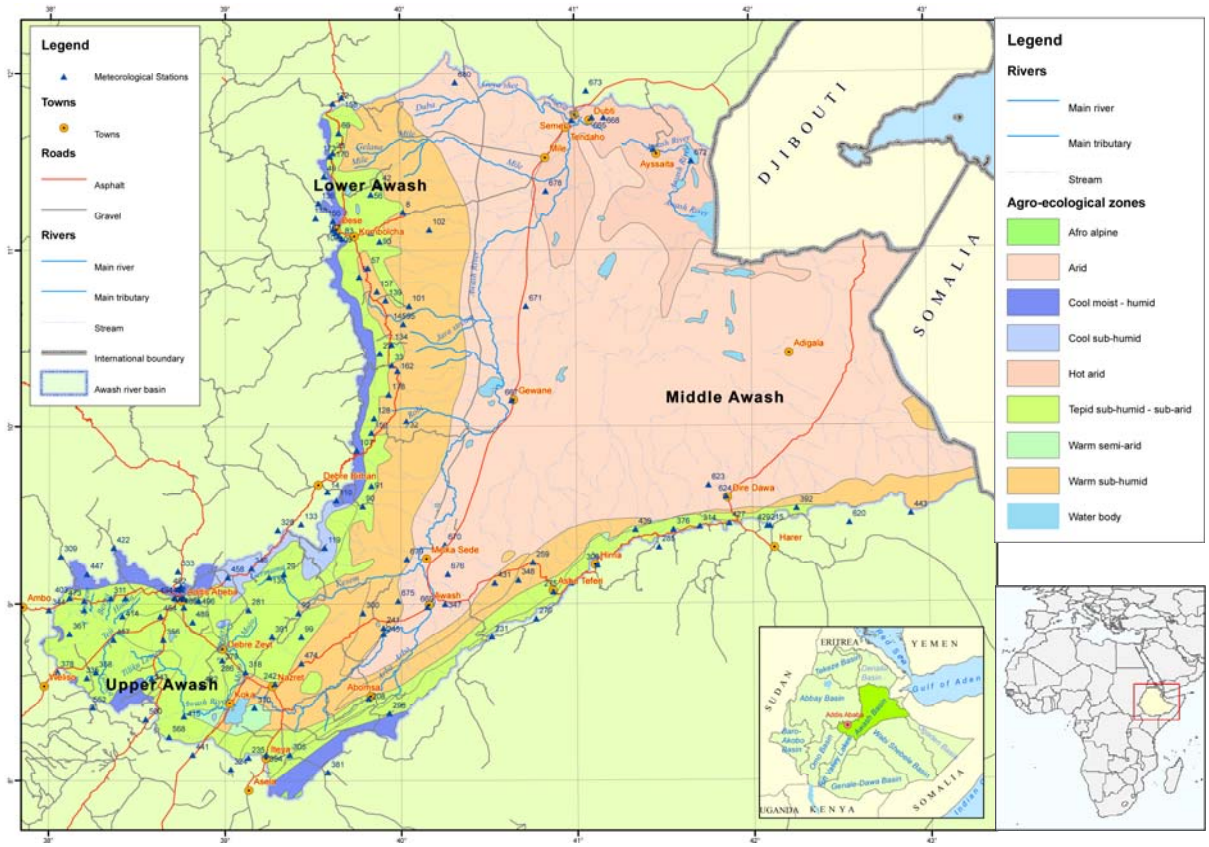

Fig. 1. Awash River Basin; source: Ministry of Water Resources, Ethiopia. Agricultural Water Management Information System [2007]

Table 1. Descriptive statistics for stations

Monthly precipitation	Station	
	Meisso	Hirna
Mean	61 mm	78 mm
Max	361 mm	459 mm

THE STANDARDIZED PRECIPITATION INDEX (*SPI*)

The standardized Precipitation Index (*SPI*) was developed by McKee *et al*. [1993]. The *SPI* index is based on precipitation alone making its evaluation relatively easy compared to other drought indices, namely the Palmer Index and the crop moisture index [Cacciamani *et al*. 2007]. In addition to the advantages mentioned earlier, a major advantage of the SPI index is that it makes it possible to describe drought on multiple time scales [Cacciamani *et al*. 2007, Mishra, Desai 2006, Tsakiris, Vangelis 2004]. The *SPI* was also determined to be the best drought index for representing the variability in East African droughts [Ntale Gan 2002], and as such was selected for this study.

The computation of the *SPI* requires fitting a probability distribution to aggregated monthly precipitation series (3, 6, 12, 24, 48 months). The probability density function is then transformed into a normal standardized index whose values classify the category of drought characterizing each place and time scale [Cacciamani *et al*. 2007]. The *SPI* can only be computed when sufficiently long (at least 30 years) and possibly continuous time-series of monthly precipitation data are available [Cacciamani *et al*. 2007]. *SPI* values can be categorized according to classes [Cacciamani *et al*. 2007]. Normal conditions are established from the aggregation of two classes: $-1 < SPI < 0$ (mild drought) and $0 \leq SPI \leq 1$ (slightly wet). *SPI* values are positive or negative for greater or less than mean precipitation, respectively. Variance from the mean is a probability indication of the severity of the flood or drought that can be used for risk assessment [Morid *et al*. 2007]. The more negative the *SPI* value for a given location, the more severe the drought. The time series of the *SPI* can be used for drought monitoring by setting application-specific thresholds of the SPI for defining drought beginning and ending times. Accumulated values of the *SPI* can be used to analyze drought severity. In this study, the SPI_SL_6 program developed by the National Drought Mitigation Centre, University of Nebraska-Lincoln, was used to compute time series of drought indices (*SPI*) for each station in the basin and for each month of the year at different time scales.

A 3-month *SPI* compares the precipitation for that period with the same 3-month period over the historical record. For example, a 3-month *SPI* at the

end of September compares the precipitation total for the July–September period with all the past totals for that same period. A 3-month *SPI* indicates short and medium term trends in precipitation and is still considered to be more sensitive to conditions at this scale than the Palmer Index [HAYES 1996]. A 3-month *SPI* can be very effective in showing seasonal trends in precipitation. The 6-month *SPI* compares the precipitation for that period with the same 6-month period over the historical record. The 6-month *SPI* indicates medium-term trends in precipitation and is still considered to be more sensitive to conditions at this scale than the Palmer Index. A 6-month *SPI* can be very effective in showing the precipitation over distinct seasons [HAYES 1996].

WAVELET DECOMPOSITION

The wavelet transform is a mathematical tool that provides a time-frequency representation of a signal in the time domain [PARTAL, KISI 2007]. In addition, wavelet analysis can often compress or denoise a signal [KIM, VALDES 2003] and thus, is an effective method for dealing with local discontinuities in a given time series. The continuous wavelet transform (CWT) is defined as the sum over all time of the signal multiplied by scaled and shifted versions of the wavelet function ψ [NASON, VON SACHS 1999]:

$$W(\tau,s)=\frac{1}{\sqrt{|s|}}\int_{-\infty}^{\infty}x(t)\psi^{*}(\frac{t-\tau}{s})dt \qquad (1)$$

where s is the scale parameter; τ is the translation and * corresponds to the complex conjugate [KIM, VALDES 2003]. The CWT is not often used for forecasting due to its complexity and long computation times. Instead, the wavelet is discretized in forecasting applications to simplify the numerical calculations. The discrete wavelet transform (DWT) requires less computation time and is simpler to implement [NASON, VON SACHS 1999]:

$$\psi_{j,k}(t)=\frac{1}{\sqrt{|s_0^j|}}\psi\left(\frac{t-k\tau_0 s_0^j}{s_0^j}\right) \qquad (2)$$

where j and k are integers that control the scale and translation respectively, while $s_0 > 1$ is a fixed dilation step [CANNAS *et al*. 2006] and τ_0 is a translation factor that depends on the aforementioned dilation step.

When conducting wavelet analysis, the number of decomposition levels that is appropriate for the data must be carefully selected. In this study, each *SPI* time series was decomposed between 1 and 9 levels. The best results were compared at all decomposition levels to determine the appropriate decomposition level. The optimal decomposition level varied between models. Once a time series was decomposed into an appropriate level, the subsequent approximation series were either chosen on their own, or they were chosen in combination with the relevant detail series, or the relevant detail series were added together without the approximation series. With most *SPI* time series, choosing just the approximation series resulted in the best forecast results. In some cases, the summation of the approximation series with a decomposed detail series yielded the best forecast results. The appropriate approximation was used as an input to the ANN models.

ANN MODELS

The ANN models used in this study have a feed forward Multi-layer perceptron (MLP) architecture which was trained with the Levenberg-Marquardt (LM) back propagation algorithm. MLPs have often been used in hydrologic forecasting due to their simplicity. MLPs consist of an input layer, one or more hidden layers, and an output layer [KIM, VALDES 2003]:

$$y`_k(t)=f_0\left[\sum_{j=1}^{m}w_{kj}.f_n(\sum_{i=1}^{N}w_{ji}x_i(t)+(w_{j0})+w_{k0}\right] \qquad (3)$$

where N is the number of samples, m is the number of hidden neurons, $x_i(t)$ = the i^{th} input variable at time step t; w_{ji} = weight that connects the i^{th} neuron in the input layer and the j^{th} neuron in the hidden layer; w_{j0} = bias for the j^{th} hidden neuron; f_n = activation function of the hidden neuron; w_{kj} = weight that connects the j^{th} neuron in the hidden layer and k^{th} neuron in the output layer; w_{k0} = bias for the k^{th} output neuron; f_0 = activation function for the output neuron; and $y_k(t)$ is the forecasted k^{th} output at time step t [KIM, VALDES 2003].

The ANN models used to forecast the *SPI* were recursive models. The input data was standardized from 0 to 1. All ANN models, without wavelet decomposed inputs, were created with the MATLAB (R.2010a) ANN toolbox. The hyperbolic tangent sigmoid transfer function was the activation function for the hidden layer, while the activation function for the output layer was a linear function. All the ANN models in this study were trained using the (LM) back propagation algorithm. The LM back propagation algorithm was chosen because of its efficiency and reduced computational time in training models [ADAMOWSKI, CHAN 2011].

There are between 3–5 inputs for each ANN model. The optimal number of input neurons was determined by trial and error, with the number of neurons that exhibited the lowest root mean square error (*RMSE*) value in the training set being selected. The inputs and outputs were standardized between 0 and

1. Traditionally, the number of hidden neurons for ANN models is selected via a trial and error method. However a study by WANAS *et al*. [1998] empirically determined that the best performance of a neural network occurs when the number of hidden neurons is equal to log (*N*), where *N* is the number of training samples. Another study conducted by MISHRA and DESAI (2006) determined that the optimal number of hidden neurons is $2n + 1$, where *n* is the number of input neurons. In this study, the optimal number of hidden neurons was determined to be between log(*N*) and $(2n+1)$. For example, if using the method proposed by WANAS *et al*. [1998] gave a result of 4 hidden neurons and using the method proposed by MISHRA and DESAI [2006] gave 7 hidden neurons, the optimal number of hidden neurons was assumed to be between 4 and 7; thereafter the optimal number was chosen via trial and error. These two methods helped establish an upper and lower bound for the number of hidden neurons. For all the ANN models, 80% of the data was used to train the models, while the remaining 20% of the data was divided into a testing and validation set with each set comprising 10% of the data.

WANN MODELS

WANN models were similar to the ANN models used in this study. However, instead of using raw *SPI* data in the input layer, WANN models used *SPI* data that had been decomposed using the 'a trous' wavelet transform algorithm. The WANN models used to forecast the SPI were also recursive models. The input data was standardized from 0 to 1. The WANN models were trained in the same way as traditional ANN models, with the exception that the inputs were made up from either the approximation series, or a combination of the approximation and detail series after the appropriate wavelet decomposition was selected. There were between 5–7 inputs for each WANN model. The optimal number of input neurons was determined by trial and error, with the number of neurons that exhibited the lowest root mean square error (*RMSE*) value in the training set being selected. The selection process for the optimal number of neurons in the hidden layer was similar to the process used for the ANN models. The inputs and outputs were standardized between 0 and 1. The data was partitioned in exactly the same way as ANN models.

SVR MODELS

SVR models adhere to the structural risk minimization principle as opposed to the empirical risk minimization principle used by conventional neural networks [VAPNIK 1995]. As a result, these models reduce the generalization error as opposed to the training error. However, these models take much longer time periods to compute compared to conventional neural networks. All SVR models were created using the OnlineSVR software created by PARRELLA [2007], which can be used to build support vector machines for regression. The data was partitioned into two sets: a calibration set and a validation set. 90% of the data was partitioned into the calibration set while the final 10% of the data was used as the validation set. Unlike neural networks the data can only be partitioned into two sets with the calibration set being equivalent to the training and testing sets found in neural networks. All inputs and outputs were standardized between 0 and 1.

All SVR models used the nonlinear radial basis function (RBF) kernel. As a result, each SVR model consisted of three parameters that were selected: gamma (γ), cost (*C*), and epsilon (ε). The γ parameter is a constant that reduces the model space and controls the complexity of the solution, while *C* is a positive constant that is a capacity control parameter, and ε is the loss function that describes the regression vector without all the input data [KISI, CIMEN 2011]. These three parameters were selected based on a trial and error procedure. The combination of parameters that produced the lowest RMSE values for the calibration data sets were selected.

RESULTS AND DISCUSSION

In the present study the ability of the aforementioned models to effectively forecast *SPI* 3 and *SPI* 6 over different lead times was evaluated. In the following sections, the forecast results for the best models in the Awash River basin are presented. The forecasts presented are from the validation data sets for time series of *SPI* 3 and *SPI* 6, which are analogous to short-term drought (agricultural drought).

For all the stations used in this study, the forecasts for *SPI* 6 were more accurate than the results for *SPI* 3. In addition, as the forecast lead time is increased from 1 to 3 months the forecast accuracy for all the stations and both *SPI* values decreased. This decrease occurred because as the forecast lead time is increased, the errors between the observed and predicted values accumulate at each lead time.

SPI 3 FORECASTS

As mentioned earlier the *SPI* forecasts were done and compared for two stations in the Awash River Basin. ANN forecasts for the Meisso station reveal that the forecast results decline considerably as the forecast lead time is increased from 1 month to 3 months. This section presents the results from the validation data sets. The *SPI* 3 forecast results for the Meisso station in terms of R^2 are 0.727 and 0.363 for lead times of 1 and 3 months, respectively. An R^2 value between 0.7–0.9 indicates a high degree of correlation, a value between 0.5–0.7 indicates a moderate

degree of correlation and a value between 0.3–0.5 indicates a low degree of correlation. For forecasts of lead times greater than one month, R^2 values above 0.2 are deemed acceptable [MISHRA *et al*. 2007]. In terms of *RMSE* the results were 0.106 and 0.103 for lead times of 1 and 3 months, respectively. *RMSE* values closer to zero indicate a high level of precision for models. As the lead time is increased the *RMSE* increases slightly, indicating that the forecasts still have a high degree of precision.

The results for SVR models are very similar to the results for ANN models. For forecasts of *SPI* 3, for both the Meisso and Hirna stations, SVR models have slightly better results than ANN models. For example, for forecasts of 1 month lead time at the Meisso station the best ANN model had results of 0.727 and 0.106 for R^2 and *RMSE*, respectively, while the best SVR model had results of 0.716 and 0.086. At the Meisso station, for the forecast of *SPI* 3 for 3 month lead time, the best SVR model had a noticeably better result in terms of R^2. The SVR model had an R^2 of 0.498 while the R^2 of the ANN model was 0.363.

Forecasts using WANN models yielded better results. In addition to more accurate results the differences between forecasts of 1 month and 3 months lead time were not as pronounced. Forecast results for 1 month lead time at the Meisso station were 0.96 and 0.029 in terms of R^2 and *RMSE*, respectively. When the forecast lead time is increased to 3 months, the results are 0.672 and 0.029, respectively. The forecast results for the Meisso station indicate, that for *SPI* 3, WANN models provide more accurate forecast results for 1 month lead time and for forecasts of 3 months lead time the results do not decline as much as those for models that do not use wavelet analysis. These trends are further exhibited by the results from the Hirna station as shown in Table 2.

Table 2. Forecast results for ANN, SVR and WANN models

Model Type	Meisso				Hirna			
	SPI 3		*SPI* 6		*SPI* 3		*SPI* 6	
	R^2	*RMSE*	R^2	*RMSE*	R^2	*RMSE*	R^2	*RMSE*
ANN L1	0.727	0.106	0.835	0.091	0.741	0.108	0.87	0.083
ANN L3	0.363	0.130	0.673	0.130	0.509	0.150	0.724	0.127
SVR L1	0.716	0.086	0.876	0.083	0.738	0.100	0.839	0.084
SVR L3	0.498	0.110	0.592	0.110	0.520	0.122	0.612	0.116
WANN L1	0.962	0.029	0.981	0.025	0.982	0.023	0.996	0.012
WANN L3	0.674	0.029	0.797	0.027	0.789	0.089	0.872	0.067

Explanations: L1 – 1-month forecast lead time; L3 – 3-month forecast lead time.
Source: own results.

SPI 6 FORECASTS

Forecast results for *SPI* 6 followed a similar pattern to the results for *SPI* 3. For the Meisso station, ANN models had forecast results of 0.835 and 0.091 in terms of R^2 and RMSE, respectively. When the forecast lead time was increased from 1 to 3 months the forecast results were 0.673 and 0.13 in terms of R^2 and *RMSE*, respectively. WANN models had more accurate results for both lead times at the Meisso station as shown in Table 2. For forecasts of 1 month lead time, the best WANN model had results of 0.981 and 0.025 in terms of R^2 and *RMSE*, respectively. When the forecast lead time was increased to 3 months, the results deteriorated to 0.797 and 0.027, respectively.

For forecasts of 1 month lead time, SVR models have very similar results to those of ANN models for both stations. However, when the forecast lead time is increased to 3 months, it seems that ANN models have slightly better results than those of SVR models. These results are presented in Table 2. An example is at the Hirna station where a *SPI* 6 forecast of 3 months lead time using the best SVR model yields results of 0.612 and 0.116 in terms of R^2 and *RMSE*, respectively, while the best ANN model has results of 0.724 and 0.127.

For a 1 month lead time, WANN models had results of 0.98 and 0.025 in terms of R^2 and RMSE, respectively. When the forecast lead time is increased to 3 months, the forecast results do not decrease as much as ANN models. For 3 months lead time, WANN models had forecast results of 0.797 and 0.027 in terms of R^2 and *RMSE*, respectively. The forecast results at the Hirna station follow the same pattern exhibited at the Meisso station. The results for the Hirna station, along with the model configurations are presented in Table 2.

DISCUSSION

The results indicate that ANN, SVR and WANN models can be used as a means of forecasting the *SPI* at 1 and 3 month lead times in the Awash River Basin. Figures 2–5 show the forecast results for ANN and WANN models. The figures illustrate how the predicted values closely mirror the observed *SPI* values. The results indicate that the use of wavelet analy-

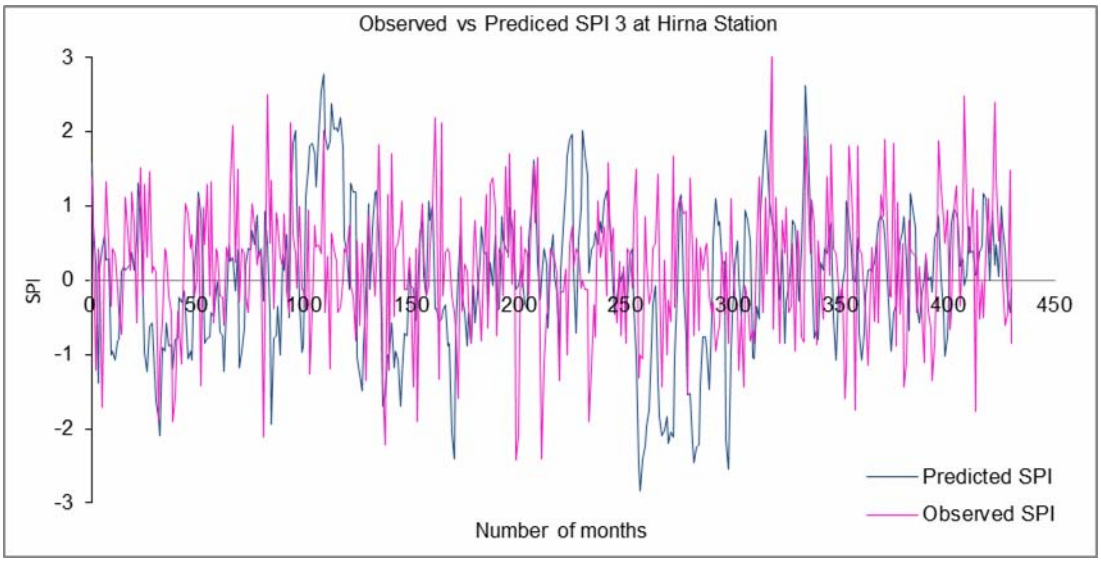

Fig. 2. *SPI* 3 forecasts using ANN model at the Hirna station; source: own results

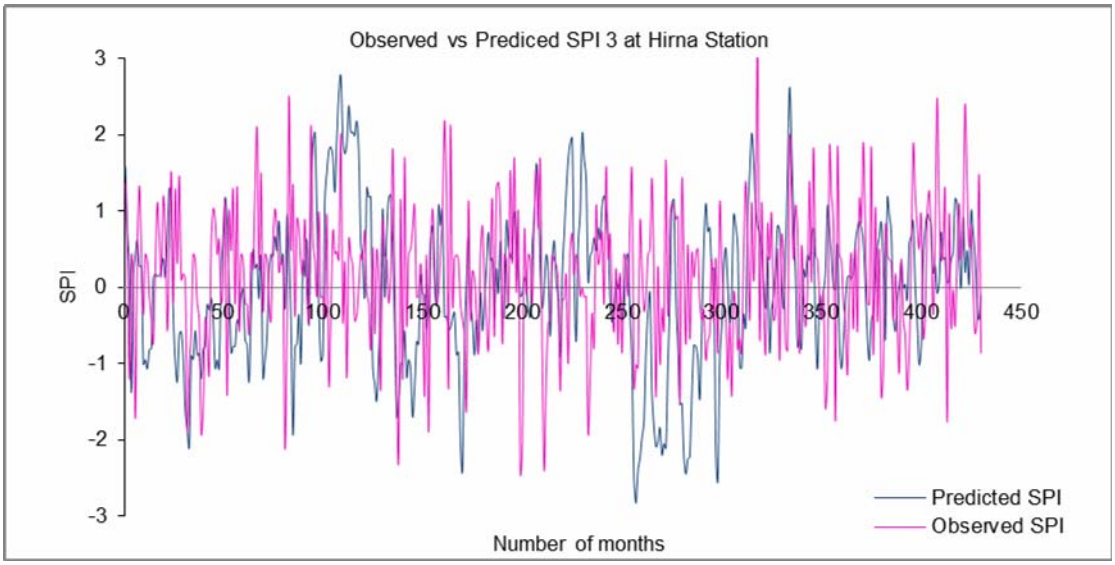

Fig. 3. *SPI* 3 forecasts using WANN models for the Hirna station; source: own results

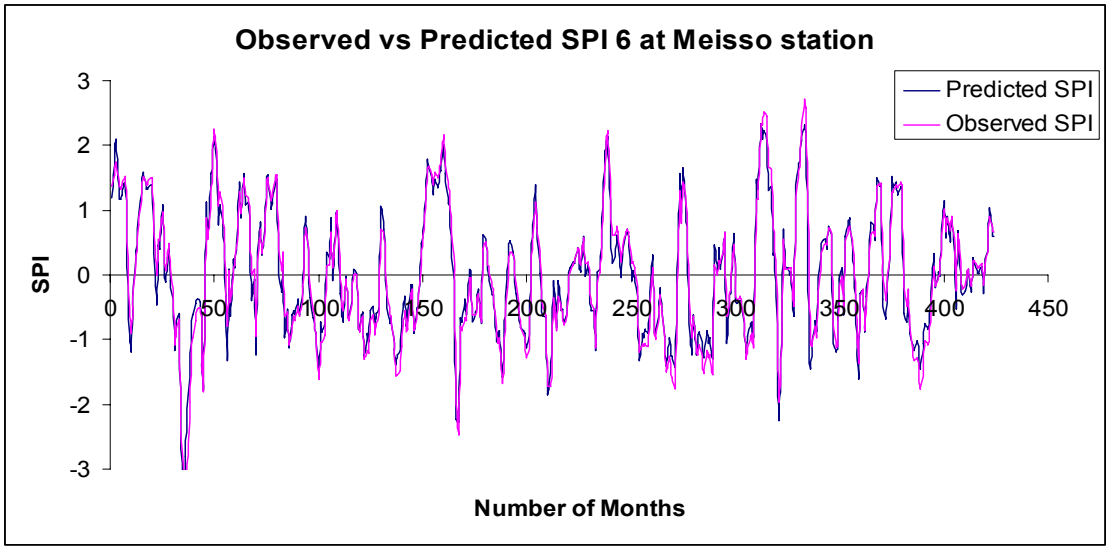

Fig. 4. *SPI* 6 forecasts using ANN models at the Meisso station; source: own results

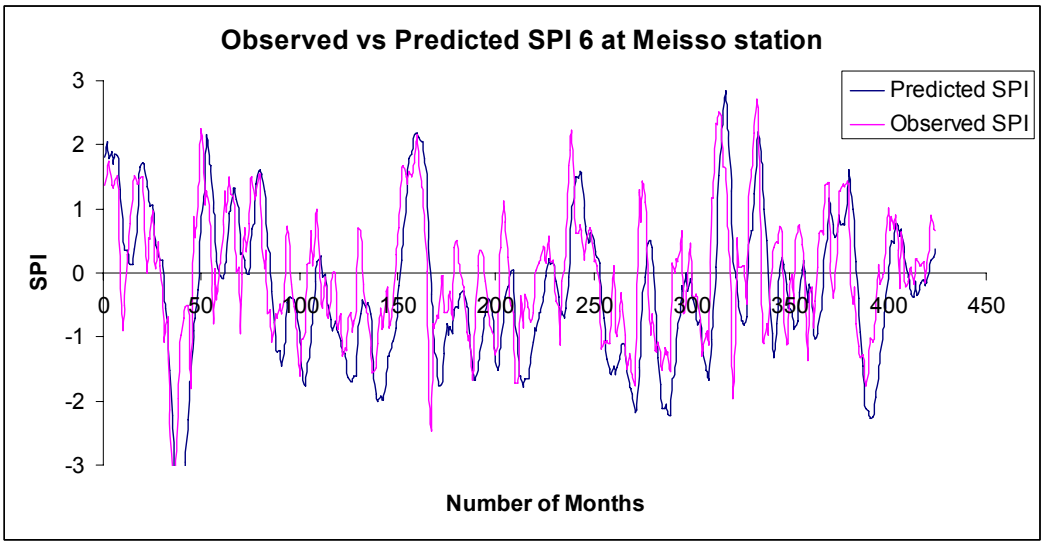

Fig. 5. *SPI* 6 forecasts using WANN models at the Meisso station; source: own results

sis as a pre-processing tool provided good forecast results for both ANN and SVR models irrespective of forecast lead time. As might be expected, the results also indicate that as the forecast lead time is increased the correlation between observed and predicted values as measured by R^2, decreases and the *RMSE* between observed and predicted values increases.

The results from all the models indicate that *SPI* 6 forecasts were more accurate than *SPI* 3 forecasts. As shown in Table 1, the results for *SPI* 6 are more accurate across all model types. Figure 4 and 5 show how the predicted *SPI* 6 values mirror those of the observed values very closely. Both *SPI* 6 and *SPI* 3 are short-term *SPI* and each new month has less impact on the period of sum precipitation [McKee *et al*. 1993]. As a result, monthly variation in precipitation has a smaller impact for *SPI* 6 compared to *SPI* 3. Since *SPI* 6 is a longer term *SPI* its sensitivity to changes in precipitation is less than that of *SPI* 3. This lack of sensitivity may explain why the forecast results for *SPI* 6 are more accurate than those of *SPI* 3. Furthermore, the use of wavelet analysis seems to have improved the results for *SPI* 3 compared to those of *SPI* 6. The inherent sensitivity that shorter term *SPI* values have to changes in precipitation within the precipitation record is why their results are not as accurate as longer term *SPI*. The use of wavelet analysis appears to reduce this sensitivity and while it improves forecasts for both *SPI* 3 and *SPI* 6, it is more beneficial for forecasts of *SPI* 3.

CONCLUSION

The ability of machine learning techniques and wavelet transforms to forecast the *SPI* drought index over 1 and 3 month lead times was investigated in this study. The results indicate that including wavelet analysis to pre-process data is an effective drought forecasting tool and improved the results of traditional ANN models. Overall, coupled wavelet-neural network (WANN) models were found to provide the best results for forecasts of *SPI* 3 and *SPI* 6 in the Awash River Basin, especially for *SPI* 6. WANN models showed a higher coefficient of determination between observed and predicted *SPI* compared to ANN and SVR models. WANN models also consistently showed lower values of *RMSE*. It is likely that the coupled models provide accurate results because pre-processing the original *SPI* time series with wavelet decompositions 'de-noises' the *SPI* time series, which subsequently allows the ANN models to model the main signal without the noise. Wavelet analysis also seems to reduce the sensitivity to changes in monthly precipitation within the *SPI* time series especially for *SPI* 3 compared to *SPI* 6. This reduction in sensitivity would be more pronounced in shorter-term *SPI* as they are inherently more sensitive to changes in monthly precipitation than longer-term *SPI*.

ACKNOWLEDGEMENTS

An NSERC Discovery and FQNRT New Researcher Grant held by Dr. Jan Adamowski were used to fund this research. The data was obtained from the Meteorological Society of Ethiopia (NMSA). Their help is greatly appreciated.

REFERENCES

Adamowski J., Chan H.F. 2011. A Wavelet Neural Network Conjunction Model for Groundwater Level Forecasting. Journal of Hydrology. Vol. 407. Iss. 1–4 p. 28–40.

Asefa T., Kemblowski M., McKee M., Khalil A. 2006. Multi-time scale stream flow 505 predicitons: The support vector machines approach. Journal of Hydrology. Vol. 318. Iss. 1–4 p. 7–16.

Bacanli U.G., Firat M., Dikbas F. 2008. Adaptive Neuro-Fuzzy Inference System for drought forecasting. Stochastic Environmental Research and Risk Assessment. Vol. 23. Iss. 8 p. 1143–1154.

BONACCORSO B., BORDI I., CANCELLIERE A., ROSSI G., SUTERA A. 2003. Spatial variability of drought: an analysis of *SPI* in Sicily. Water Resources Management. Vol. 17. Iss. 4 p. 273–296.

BARROS A., BOWDEN G. 2008. Toward long-lead operational forecasts of drought: An experimental study in the Murray-Darling River Basin. Journal of Hydrology. Vol. 357. Iss. 3–4 p. 349–367.

CACCIAMANI C., MORGILLO A., MARCHESI S., PAVAN V. 2007. Monitoring and forecasting drought on a regional scale: Emilia-Romagna Region. In: Methods and tools for drought Analysis and management. Eds. G. Rossi, T. Vega, B. Bonaccorso. Water Science and Technology Library. Vol. 62 (1) p. 29–48.

CANNAS B., FANNI A., SIAS G., TRONCI S., ZEDDA M.K. 2006. River flow forecasting using neural networks and wavelet analysis. Proceedings of the European Geosciences Union.

CUTORE P., DI MAURO G., CANCELLIERE A. 2009. Forecasting Palmer Index using neural networks and climatic indexes. Journal of Hydrologic Engineering. Vol. 14. No. 6 p. 588–595.

EDOSSA D.C., BABEL M.S., GUPTA A.D. 2010. Drought analysis on the Awash River Basin, Ethiopia. Water Resource Management. Vol. 24. Iss. 7 p. 1441–1460.

HAYES M. 1996. Drought indexes. National Drought Mitigation Center, University of Nebraska–Lincoln, p. 7 (available from University of Nebraska–Lincoln, 239LW Chase Hall, Lincoln, NE 68583).

KARAMOUZ M., RASOULI K., NAZIL S. 2009. Development of a Hybrid Index for Drought Prediction: Case study. Journal of Hydrologic Engineering. Vol. 14. No. 6 p. 617–627.

KHAN M.S., COULIBALY P. 2006. Application of support vector machine in lake water level prediction. Journal of Hydrologic Engineering. Vol. 11. No. 3 p. 199–205.

KIM T., VALDES J.B. 2003. Nonlinear model for drought forecasting based on a conjunction of wavelet transforms and neural networks. Journal of Hydrologic Engineering. Vol. 8. No. 6 p. 319–328.

KISI O., CIMEN M. 2009. Evapotranspiration modelling using support vector machines. Hydrological Science Journal. Vol. 54. Iss. 5 p. 918–928.

KISI O., CIMEN M. 2011. A wavelet-support vector machine conjunction model for monthly streamflow forecasting. Journal of Hydrology. Vol. 399. Iss. 1–2 p. 132–140.

MAITY R., BHAGWAT P.P., BHATNAGAR A. 2010. Potential of support vector regression for prediction of monthly streamflow using endogenous property. Hydrological Processes. Vol. 24. Iss. 7 p. 917–923.

MARJ A.F., MEIJERINK A.M. 2011. Agricultural drought forecasting using satellite images, climate indices and artificial neural network. International Journal of Remote Sensing. Vol. 32. No. 24 p. 9707–9719.

MCKEE T.B., DOESKEN N.J., KLEIST J. 1993. The relationship of drought frequency and duration to time scales. 8th Conference on Applied Climatology. 17-22 January 1993, Anaheim, California. American Meteorological Society, Anaheim, CA.

Ministry of Water Resources. 2007. The Awash River Basin. http://www.mowr.gov.et/AWMISET/images/Awash_agroecologyv3.pdf. Accessed 06-June-2013

MISHRA A.K., SINGH V.P. 2010. A review of drought concepts. Journal of Hydrology. Vol. 391. Iss. 1–2 p. 202–216.

MISHRA A.K., DESAI V.R. 2006. Drought forecasting using feed-forward recursive neural network. Ecological Modelling. Vol. 198. No. 1–2 p. 127–138.

MISHRA A.K., DESAI V.R., SINGH V.P. 2007. Drought forecasting using a hybrid stochastic and neural network model. Journal of Hydrologic Engineering. Vol. 12. Iss. 6 p. 626–638.

MORID S., SMAKHTIN V., BAGHERZADEH K. 2007. Drought forecasting using artificial neural networks and time series of drought indices. International Journal of Climatology. Vol. 27. Iss. 15 p. 2103–2111.

NASON G.P., VON SACHS R. 1999. Wavelets in time-series analysis. Philosophical Transactions of the Royal Society A: Mathematical, Physical and Engineering Sciences. Vol. 357. No. 1760 p. 2511–2526.

NTALE H.K., GAN T.Y. 2003. Drought indices and their application to East Africa. International Journal of Climatology. Vol. 23. Iss. 11 p. 1335–1357.

PARRELLA F. 2007. Online support vector regression. Master Thesis, University of Genoa.

PARTAL T., KISI O. 2007. Wavelet and neuro-fuzzy conjunction model for precipitation forecasting. Journal of Hydrology. Vol. 342. Iss. 1–2 p. 199–212.

TIWARI M.K., CHATTERJEE C. 2010. Development of an accurate and reliable hourly flood forecasting model using wavelet-bootstrap-ANN (WBANN) hybrid approach. Journal of Hydrology. Vol. 394. Iss. 3–4 p. 458–470.

TSAKIRIS G. VANGELIS H. 2004. Towards a Drought Watch System based on spatial SPI. Water Resources Management. Vol. 18. Iss. 1 p. 1–12.

VAPNIK V. 1995. The nature of statistical learning theory. New York, USA. Springer Verl. ISBN-10: 0387987800 pp. 334.

WANG W.C., CHAU K.W., CHENG C.T., QIU L. 2009. A comparison of performance of several artificial intelligence methods for forecasting monthly discharge time series. Journal of Hydrology. Vol. 374. Iss. 3–4 p. 294–306.

WANAS N., AUDA G., KAMEL M.S., KARRAY F. 1998. On the optimal number of hidden nodes in a neural network. In: Proceedings of the IEEE Canadian Conference on Electrical and Computer Engineering. Michigan. IEEE p. 918–921.

Anteneh BELAYNEH, Jan ADAMOWSKI

Prognozowanie suszy z wykorzystaniem automatycznych samouczących się metod

STRESZCZENIE

Słowa kluczowe: *analiza falowa, prognoza suszy, regresja wektorowa, rolnictwo, SPI, sztuczna sieć neutronowa*

Efektywna gospodarka rolna, uzyskanie dużych plonów wymaga prowadzenia działań w celu ograniczenia niekorzystnego wpływu suszy. Ważnym czynnikiem ograniczania skutków suszy jest efektywna i możliwie precyzyjna metoda przewidywania suszy. W artykule przedstawiono trzy metody prognozowania suszy w okresach krótkoterminowych, które zostały zastosowane w zlewni rzeki Awash w Etiopii. Do kwantyfikacji suszy zastosowano wskaźnik standaryzowanego opadu (*SPI*). Zastosowane zostały następujące samouczące się metody: sztuczne sieci neuronowe (ANNs), regresje wektorowe (SVR) oraz połączenie ANNs z analizą falową (WA), którą zastosowano do wstępnej obróbki danych. Ocenę prognozy dokonano stosując dwa mierniki – *RMSE* i R^2. Na podstawie obliczeń stwierdzono, że połączona metoda analizy falowej z siecią neutronową (WA-ANN) jest najdokładniejsza w prognozowaniu wartości *SPI* 3 (3-miesięczne *SPI*) i *SPI* 6 (6-miesięczne *SPI*) w okresie 1 i 3 miesiące naprzód w zlewni rzeki Awash.

.